Geochemical Perspectives Letters

Morphology dominated rapid oxidation of framboidal pyrite

R. Du, H. Xian, X. Wu, J. Zhu, J. Wei, J. Xing, W. Tan, H. He

Supplementary Information

The Supplementary Information includes:

- Materials and Methods
- Supplementary Text: Calculation of specific surface area; surface species on the microscopic pyrite
- Tables S-1 to S-3: S 2*p* peak parameters and chemical states of oxidised pyrites, S/Fe ratios derived from X-ray photoelectron spectroscopy (XPS) survey spectra at different oxidation intervals, and a comparison of oxidation rates of the samples.
- Figures S-1 to S-3: S 2*p* spectra and Fe $2p_{3/2}$ XPS spectra of oxidised Py-tc, Py-co and Py-to surfaces and the kinetic data normalised by the SSAs of the three samples.
- Supplementary Information References

Materials and Methods

Preparation of microscopic pyrite

Highly pure microscopic pyrite samples were synthesised using a polymer-assisted hydrothermal method which was modified after Wang *et al.* (2010). The process was performed in a glove box (MIKROUNA) fulfilled with high-pure nitrogen (>99.99 %), 21 mL polyvinyl alcohol solution (4.4 *wt.* %) and 0.45 g polyvinylpyrrolidone were dissolved in 39 mL water, then 0.4 g $FeCl_2 \cdot 4H_2O$ was added to this solution under constant stirring to form a homogeneous mixture. 10 mL NaOH (0.7 M) was added dropwise into the mixture, and finally 0.4 g Sulfur powder was added to the solution under magnetic stirring for 1 hour. By appropriately increasing the amount of NaOH (0.7 M) from 10 mL to 11 mL, microcrystalline pyrite with different morphologies containing {100} and {111} crystal facets finally can be synthesised. The above reagents are of analytical grade. The mixture was sealed in a Teflon-lined stainless-steel autoclave (70 % filled), and maintained at 453 K for 12 h, then cooled to room temperature naturally. The products were washed 3 times with Milli-Q water and 3 times with anhydrous ethanol. The collected samples were dried at 60° under vacuum, and then stored in the glove box with nitrogen atmosphere.

Oxidation experiments

The samples possessing similar morphology with framboidal pyrite microscopic crystals were used to conduct oxidation experiments in 77 $_{Rh}$% air. Glass slides with covered pyrite film were employed to the oxidation experiments, which was prepared in the oxygen-insulated glove box. The pyrite films were prepared by dropping suspension on glass slides, the suspension composed of the pyrite samples and ethanol. The oxidation experiments were carried out in an airtight homemade reaction cell at room temperature. Saturated NaCl solution was used to control the humidity condition, providing a relative humidity of 77 $_{Rh}$% throughout the experiments.

Characterisation

The X-ray diffraction (XRD) patterns were recorded on a Bruker D8 ADVANCE X-ray diffractometer with a Ni filter and Cu Kα radiation source, which were operated at a generator voltage of 40 kV and a current of 40 mA. The chemical composition and morphology of the samples were analysed on a MIRA3 TESCAN field emission scanning electron microscope (FESEM) equipped with the energy dispersive spectrometry (EDS). The working distance of the EDS analysis was set at 6.5 mm. Thin sections of natural pyrite samples were prepared for scanning electron microscopy (SEM) observations using a Phenom XL SEM equipped with a back-scattered electron (BSE) detector. X-ray photoelectron spectroscopic (XPS) analysis on a Thermo Scientific K-alpha spectrometer with a base pressure of 10^{-8} mbar and an aluminium Kα source (1486.8 eV). The spectra were processed using the Thermo Avantage analysis software with smart backgrounds and peaks with mixed Lorentz-Gaussian shapes.

Supplementary Text

Calculation of specific surface area

Because the limited amount of synthesised samples restricted the use of the N_2 adsorption BET method to determine their SSA, the SSAs of the pyrite samples were estimated based on geometry, as follows:

$$S = s / V\rho,$$

where S is the SSA, s and V are the surface area and volume of the grains, respectively, and ρ is the density of pyrite (5 g/cm^3). The geometric lengths required in the calculations were derived from the average value of the statistical measurements from a series of FESEM micrographs (Fig. 1j–l). According to the geometric model, the SSAs were 2.54, 1.96 and 1.83 m^2/g for the Py-tc, Py-co and Py-to samples, respectively.

Surface species on the microscopic pyrite

S 2*p* and Fe2$p_{3/2}$ XPS spectra are utilized to characterize surface states of pyrite before and after oxidation (Herbert *et al.*, 2014; Zhu *et al.*, 2018; Xian *et al.*, 2019). From XPS S 2*p* spectra of the pyrite samples before and after oxidization for 84 hours (Fig. S-1), two doublets, with maxima at 162.50 and 161.80 eV are assigned to the bulk sulfur dimer (S_2^{2-}-bulk) and the surface sulfur dimer (S_2^{2-}-surface), respectively. The tail feature at 164.40 eV is generated by the core-hole effect in pyrite (Herbert *et al.*, 2014). Two doublets, with maxima at 166.60 and 168.20 eV are assigned to the thiosulphate ($S_2O_3^{2-}$) and sulphate (SO_4^{2-}) on the surface of oxidised pyrite, respectively. The results (Table S-1) showed that thiosulphate only present at the initial stage of pyrite oxidation, thereby indicating that thiosulfate rapidly converts to sulphate. From XPS Fe2$p_{3/2}$ spectra of the pyrite samples before and after oxidisation for 84 hours (Fig. S-2), the low spin bulk Fe at 706.60 eV and two surface Fe states were observed. One surface Fe state is a quadruplet with a minimum at 707.20 eV, and the other one is a triplet with a minimum at 708.50 eV. A quadruplet with minima at 710.80 eV is assigned to Fe (III)-O type species. The peaks of sulphate and iron oxyhydroxides increase with the oxidation time (Figs. S-1 and S-2), indicating the increase of their content on the surface of pyrite samples.

Supplementary Tables

Table S-1 S 2*p* peak parameters and chemical states of oxidised pyrites.

Samples	Species	△E_B/eV	Percentage of species detected					
			0 hr	6 hr	12 hr	36 hr	60 hr	84 hr
Py-tc	Bulk S Doublet	0 1.2	75.58	77.01	74.92	73.09	71.57	70.93
	Surf S Doublet	-0.7 0.5	13.82	13.98	13.45	12.43	12.06	11.59
	CH	2.18	10.54	9.00	11.41	12.07	11.61	10.74
	Sulfate Doublet	5.7 6.9	0.00	0.00	0.22	2.41	4.76	6.73
	Thiosulfate Doublet	**4.05 5.25**	**0.07**	**0.00**	**0.00**	**0.00**	**0.00**	**0.00**
Py-co	Bulk S Doublet	0 1.2	74.33	74.68	74.41	72.87	69.58	67.88
	Surf S Doublet	-0.7 0.5	13.84	13.56	13.23	13.15	11.91	11.63
	CH	2.18	11.79	11.12	11.09	11.13	11.58	11.67
	Sulfate Doublet	5.7 6.9	0.00	0.11	0.83	2.63	6.83	8.81
	Thiosulfate Doublet	**4.05 5.25**	**0.03**	**0.53**	**0.45**	**0.23**	**0.11**	**0.00**
Py-to	Bulk S Doublet	0 1.2	74.31	75.13	73.42	71.48	64.39	65.01
	Surf S Doublet	-0.7 0.5	14.20	13.83	13.47	12.97	11.98	11.75
	CH	2.18	11.49	10.79	11.87	11.28	12.87	12.09
	Sulfate Doublet	5.7 6.9	0.00	0.00	0.84	4.14	10.76	11.15
	Thiosulfate Doublet	**4.05 5.25**	**0.00**	**0.25**	**0.40**	**0.12**	**0.00**	**0.00**

Table S-2 S/Fe ratios derived from X-ray photoelectron spectroscopy (XPS) survey spectra at different oxidation intervals.

Samples	S/Fe ratio (XPS survey spectra)					
	0 hr	6 hr	12 hr	36 hr	60 hr	84 hr
Py-tc	3.29	3.27	3.47	3.69	3.94	4.12
Py-co	3.38	3.52	3.55	3.61	3.40	3.42
Py-to	3.71	3.58	3.72	4.14	3.92	3.83

Table S-3 Comparison of oxidation rates of Py-tc, Py-co and Py-to.

Samples	Rate (mol O^2/m^2s)	
	$r_{S\ 2p}$	$r_{Fe\ 2p3/2}$
Py-tc	$(5.595 \pm 0.3520) \times 10^{-9}$	$(6.768 \pm 0.4287) \times 10^{-9}$
Py-co	$(7.987 \pm 0.4873) \times 10^{-9}$	$(9.340 \pm 1.1145) \times 10^{-9}$
Py-to	$(1.024 \pm 0.1029) \times 10^{-8}$	$(1.385 \pm 0.1548) \times 10^{-8}$

Calculation methods refer to the literature (Zhu *et al.*, 2018).

Supplementary Figures

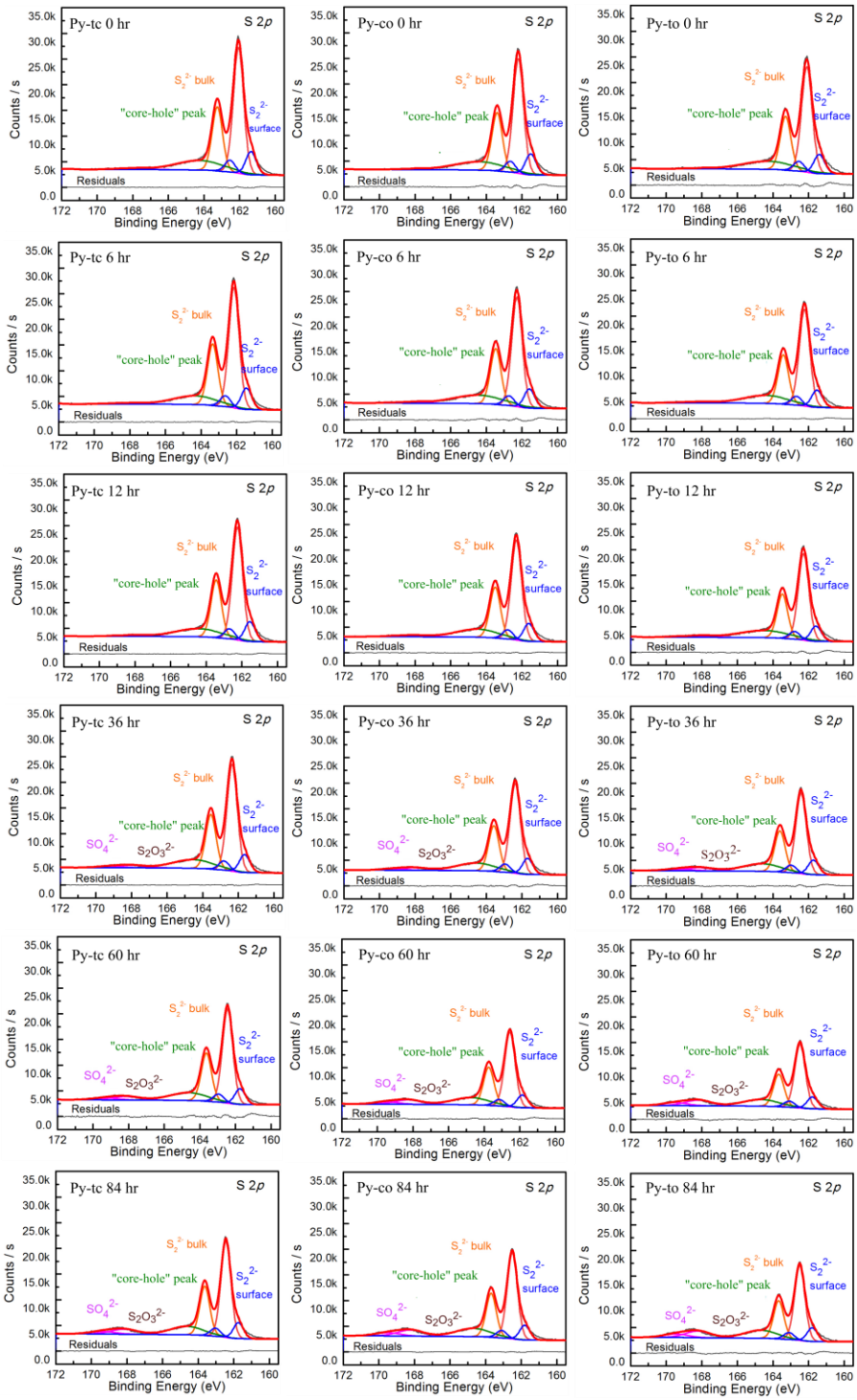

Figure S-1 S2*p* X-ray photoelectron spectroscopy spectra of pyrite Py-tc (truncated cubic pyrite) , Py-co (cubo-octahedral pyrite), and Py-to (truncated octahedral pyrite) surfaces oxidised in air with a relative humidity of 77 % at intervals of 0, 6, 12, 36, 60 and 84 hr.

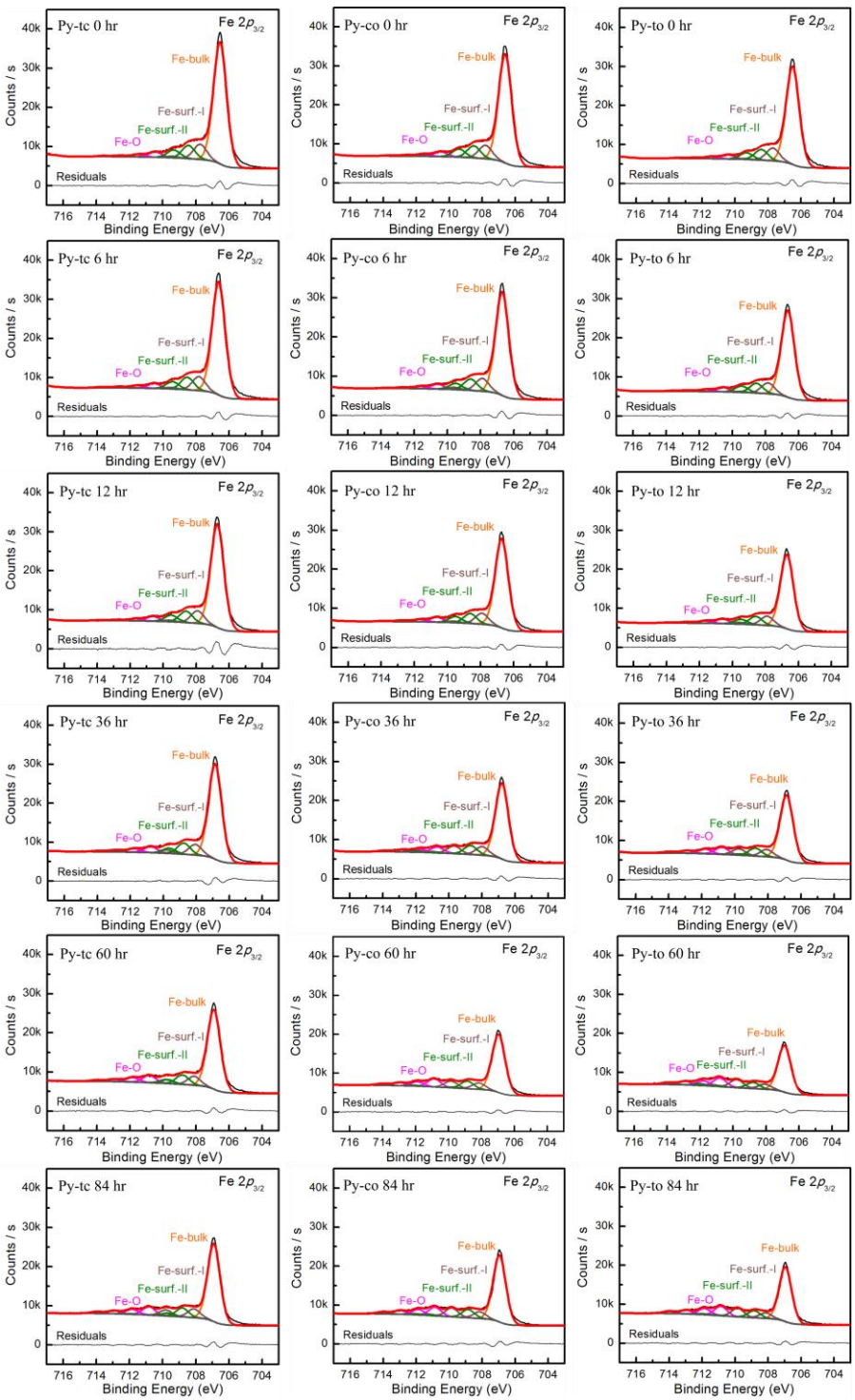

Figure S-2 Fe $2p_{3/2}$ X-ray photoelectron spectroscopy spectra of pyrite Py-tc (truncated cubic pyrite) , Py-co (cubo-octahedral pyrite), and Py-to (truncated octahedral pyrite) surfaces oxidised in air with a relative humidity of 77 % at intervals of 0, 6, 12, 36, 60 and 84 hr.

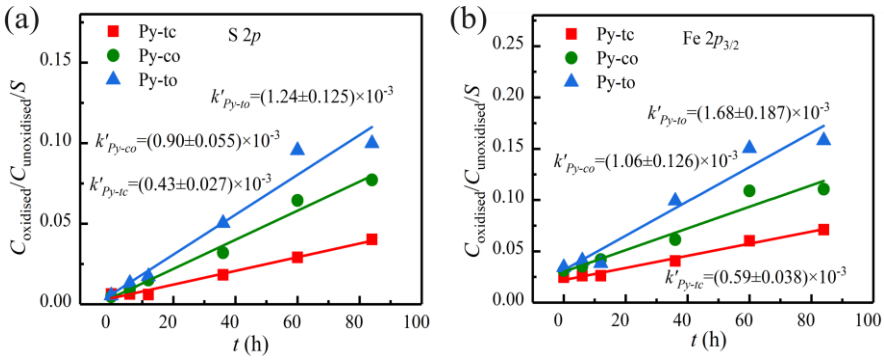

Figure S-3 The kinetic data normalised by SSA of the three samples. *k´ vs*. oxidation time (*t*) from S 2*p* **(a)** and Fe $2p_{3/2}$ **(b)** XPS spectra of pyrite Py-tc, Py-co and Py-to oxidised surfaces. *k´* is the concentraition ratio of oxygen-containing species to unoxidised species ($C_{oxidised}/C_{unoxidised}$)/SSAs.

Supplementary Information References

Herbert, F.W., Krishnamoorthy, A., Ma, W., Van Vliet, K.J., Yildiz, B. (2014) Dynamics of point defect formation, clustering and pit initiation on the pyrite surface. *Electrochimica Acta* 127, 416–426.

Wang, D., Wang, Q., Wang, T. (2010) Controlled growth of pyrite FeS 2 crystallites by a facile surfactant-assisted solvothermal method. *CrystEngComm* 12, 755–761.

Xian, H., He, H., Zhu, J., Du, R., Wu, X., Tang, H., Tan, W., Liang, X., Zhu, R., Teng, H. (2019) Crystal habit-directed gold deposition on pyrite: Surface chemical interpretation of the pyrite morphology indicative of gold enrichment. *Geochimica et Cosmochimica Acta* 264, 191–204.

Zhu, J., Xian, H., Lin, X., Tang, H., Du, R., Yang, Y., Zhu, R., Liang, X., Wei, J., Teng, H., He, H. (2018) Surface structure-dependent pyrite oxidation in relatively dry and moist air: Implications for the reaction mechanism and sulfur evolution. *Geochimica et Cosmochimica Acta* 228, 259–274.